11-19-2020

Easy-Processable and Aging-Free All-Polymer Polysiloxane Composites

Liyang Shen
Iowa State University, lshen@iastate.edu

Tung-Ping Wang
Iowa State University, wangtp@iastate.edu

Shailja Goyal
Iowa State University, sgoyal@iastate.edu

See next page for additional authors

Easy-Processable and Aging-Free All-Polymer Polysiloxane Composites

Abstract

Here, we report all-polymer polysiloxane composites that overcome the long-standing processing problems of silica-reinforced silicone rubbers. Polystyrene fillers are dispersed with styrene/dimethylsiloxane symmetric diblock and triblock copolymers that control the filler morphology, filler–matrix interactions, and filler–filler interactions. Surprisingly, the composites not only rival the traditional silica-reinforced polysiloxane in mechanical properties of cured materials but also have better processability and stability than the silica-filled compound before curing. Large amplitude oscillatory shear experiments demonstrate that the triblock copolymer addition strongly affects the rheological properties. We hypothesize that the bridges and entangled loops that were formed by the triblock copolymer can connect different PS domains to provide additional reinforcement. The aging effect that originates from PDMS chain adsorption on the filler particle surface is also avoided because of the thermodynamic repulsion between PS and PDMS phases.

Keywords

polysiloxane composites, block copolymers, polystyrene-b-polydimethylsiloxane, mechanical reinforcement, large amplitude oscillatory shear, transmission electron microscopy

Disciplines

Polymer and Organic Materials

Authors

Liyang Shen, Tung-Ping Wang, Shailja Goyal, Ting-Han Lee, Fang-Yi Lin, Sabrina Torres, Thomas Robison, and Eric W. Cochran

Easy-processable and Aging-free All-polymer Polysiloxane Composites

Liyang Shen,[†] Tung-ping Wang,[†] Shailja Goyal,[†] Ting-Han Lee,[†] Fang-Yi Lin,[†] Sabrina Torres,[‡] Thomas Robison,[‡] and Eric W. Cochran[*,†]

†Department of Chemical and Biological Engineering, Iowa State University, Ames, Iowa 50011, United States

‡Kansas City National Security Campus, 14520 Botts Road, Kansas City, Missouri 64147, United States

E-mail: ecochran@iastate.edu

Abstract

Here we report all-polymer polysiloxane composites that overcome the long-standing processing problems of silica-reinforced silicone rubbers. Polystyrene fillers are dispersed with styrene/dimethylsiloxane symmetric diblock and triblock copolymers that control the filler morphology, filler-matrix interactions, and filler-filler interactions. Surprisingly, the composites not only rival the traditional silica-reinforced polysiloxane in mechanical properties of cured materials, but also have better processability and stability than the silica filled compound before curing. Large amplitude oscillatory shear experiments demonstrate that the triblock copolymer addition strongly affects the rheological properties. We hypothesize that the bridges and entangled loops that formed by the triblock copolymer can connect different PS domains to provide additional reinforcement. The aging effect that originates from PDMS chain adsorption on the filler particle surface is also avoided because of the thermodynamic repulsion between PS and PDMS phases.

Keywords

polysiloxane composites, block copolymers, polystyrene-b-polydimethylsiloxane, mechanical reinforcement, large-amplitude-oscillatory-shear, transmission electron microscopy

Introduction

Fillers are usually essential to elastomeric materials for various reasons, most often including mechanical reinforcement. In polysiloxane elastomers such as polydimethylsiloxane (PDMS) the mechanical properties are especially poor without reinforcing fillers.[1] Fumed silica is a widely used filler for polysiloxanes because of the hydrodynamic effect brought by the inclusion of rigid particles as well as favorable filler-filler and filler-matrix interactions.[2,3] The filler-filler interactions derive from the bonding within aggregates and the physical force between agglomerates, which are clusters of aggregates.[4,5] The filler-polymer interactions originate from the physical adsorption when matrix polymer chains are adsorbed by the surface of particle,[1] polymer chain bridges between particles,[6] and hydrogen bonding between the silica hydroxyl groups and polysiloxane chains.[7]

However, these strong interactions also bring some side effects. The addition of silica increases the compound viscosity dramatically, even reaching solid-like behavior at sufficient filler content.[8] Strongly favorable enthalpic interactions promote the adsorption of polymer chains on the filler surface, yielding a thin layer known as "bound rubber"[4] that is so strongly bound that it cannot be removed by solvent.[9] The adsorption process is slow, requiring several days to months to equilibrate. During this equilibration period the viscosity/dynamic modulus of the precured compounds changes drastically accompanied with filler agglomeration.[1,4,6,10–13] These phenomena are known as aging effects; crepe hardening refers to high molecular weight polysiloxane matrices (gum silicone),[1,10,13] while softening can occur in low molecular weight polysiloxane matrices (liquid silicone).[8,10–12] Aging effects are currently mitigated through plasticizers[14] and silica pretreatments[15] to weaken the matrix-filler in-

teraction. These processing difficulties and storage issues of the precured compounds bring inconvenience, raise production cost, and impact reproducibility.

All-polymer polysiloxane blends and alloys have been sought after to improve processability and eliminate aging effects. Glassy and semicrystalline polymers can potentially provide sufficient mechanical reinforcement to polysiloxanes. Several groups have prepared PDMS/glassy thermoplastic blends via in-situ radical copolymerization of monomer in presence of PDMS matrix, improving the mechanical properties of PDMS by incorporating the polystyrene (PS)[16–20] and other glassy polymers.[21,22] Although the in-situ polymerization strategy can yield relatively small fillers, the immiscibility and large viscosity difference make it almost impossible to obtain uniform filler dispersion. In addition, the immiscibility between PDMS and PS heavily destabilizes the morphology and precludes strong interfacial adhesion,[23–25] limiting the improvement of mechanical properties. The modifications can be also achieved via interpenetrating polymer networks.[26–28] Adding block copolymers (BCPs) is a classical solution to reduce the interfacial energy amongst otherwise incompatible polymers. The well-known thermoplastic elastomers, such as poly(styrene-butadiene-styrene) or PS-PDMS-PS, are block copolymers composed of hard and soft polymer blocks.[29–31] Self-assembly yields microphase-separated structures with plastically deformable microdomains that serve as physical crosslinks; careful design of composition and molecular weight allows tailored mechanical properties. Alternatively, soft-hard-soft block sequences like PDMS-PS-PDMS triblock copolymers behave as ductile plastics with 50 wt% polystyrene, while at 30 wt% polystyrene there is increased elasticity but weaker strength and a significant yield point.[32,33] Thus as neat materials, siloxane-based BCPs can achieve desirable mechanical properties without chemical crosslinking, although tradeoffs like cost and processability limit their practical utility.

Alternatively, BCPs can serve as fillers or additives in homopolymer matrices, which can be more effective and cost-efficient compared to neat BCP matrices. Recently, we reported the potential of a PS-PDMS diblock copolymer filler in PDMS thermosets, which displays

comparable mechanical performance to silica-filled controls.[34] Further, BCPs can be used even more sparingly as an additive to stabilize the interfaces in PS/PDMS homopolymer blends. For example, in thermoplastic PDMS-filled PS matrices, it has been demonstrated that < 10 wt% PS-PDMS is sufficient to reduce PDMS filler size and improve dispersion.[35,36] Conversely, glassy homopolymer reinforcing fillers, stabilized via BCP compatibilizers, may be a preferential strategy to optimize the mechanical properties of polysiloxane composites. In this work, we adopt this strategy to achieve PS homopolymer-reinforced PDMS thermoset elastomers. The PS homopolymer phases are dispersed primarily with symmetric PDMS-PS block copolymers to encourage the formation of homopolymer-filled micelles with strong interfaces. Symmetrical diblock copolymers were reported to be more efficient in compatibilization of homopolymer blends than asymmetrical diblock copolymers, which tend to form micelles, whereas the symmetrical diblock copolymers tend to reside at the interface between the homopolymer domains.[37,38] Furthermore, we illustrate that under certain conditions the addition of PS-PDMS-PS triblock copolymer can promote filler-filler interactions. We hypothesize that the triblock copolymers form bridges that connecting disparate PS domains, increasing the efficacy of the mechanical reinforcement effect. The aging effects that originate from PDMS chain adsorption on the filler particle surface in silica-filled systems should be also avoided because of the immiscibility between PS and PDMS. As demonstrated below, the all-polymer polysiloxane composites reinforced by polystyrene and its block copolymers show superior mechanical properties compared to the traditional silica-modified analogs, as well as the better processability and stability before the thermal curing process.

EXPERIMENTAL SECTION

Materials

Cyclohexane (HPLC, Fisher Scientific), tetrahydrofuran (THF) (HPLC, Fisher Scientific) and styrene (99%, Sigma-Aldrich) were stored in argon-purged tanks and purified through

alumina columns.[39] Hexamethylcyclotrisiloxane (D_3) (98%, Sigma-Aldrich) dissolved in cyclohexane (0.6g D_3/mL) was distilled at 150 °C under argon to remove high boiling point impurities, remained over activated molecular sieves (20 m/v) for two days, and underwent three freeze-pump-thaw cycles before addition. All operations and transports were conducted with a Schlenk line. Sec-butyllithium 1.4 M in cyclohexane, trimethylchlorosilane (98%) and dichlorodimethylsilane (99.5%) were purchased from Sigma-Aldrich and used as received. Vinyl-terminated PDMS (DMS-V31), the crosslinking agent methylhydrosiloxane-dimethylsiloxane copolymer (HMS-301) and platinum catalyst (SIP6832.2) were purchased from Gelest and used as received. Fumed silica (CAB-O-SIL, MS-75D) was generously provided by Cabot Corporation. Polystyrene homopolymer (homoPS, H) was purchased from Sigma-Aldrich and used as received.

Synthesis of PS-PDMS diblock copolymer and PS-PDMS-PS triblock copolymer

To control the molecular weight precisely, anionic polymerization was adopted to synthesize volume symmetric PS-PDMS diblock copolymer (diBCP, D) with narrow molecular weight distribution.[40–43] The synthetic routes are shown in **Scheme S1**. PS-PDMS-PS triblock copolymer (triBCP, T) was generated by coupling the diblock by the bifunctional chlorosilane. The polymerization of polystyrene was initiated by sec-butyllithium and continued at 40 °C for 4 hours. Before the second monomer addition, a small aliquot was withdrawn by a syringe, and terminated by degassed methanol for analysis. The temperature was then decreased to 25 °C, and two-fold excess D_3 was added to prevent side reactions and left to stand for 12 h. Then, THF was added as polarity promoter to make a 50% (v/v) mixture. After 4 h, for diBCP, the reaction was terminated by trimethylchlorosilane, while for triBCP, the reaction was terminated by dichlorodimethylsilane dropwise and left to stand for 24 h at 0 °C. The solution was precipitated by methanol, for three times. The final product was dried under vacuum.

Preparation of PDMS composites and characterizations

The raw materials of vinyl-terminated PDMS matrix, crosslinking agent (4 phr) and filler were mixed at 160 °C, 200 rpm for 30 minutes in twin-screw micro-compounder (DACA Instruments, USA). Air bubbles were removed under vacuum. After the platinum catalyst (200 ppm) was added and mixed, the mixture was put under vacuum again. The final step was the crosslinking reaction shown in **Scheme S2** by compression molding at 5000 lbs, 150 °C for 3 h.

Gel permeation chromatography (GPC) measurements were running at 70 °C, 0.8 mL/min in integrated Waters Acquity UPLC system. The concentration of samples was 5 mg/mL and ethyl acetate was used as eluent. PS standards were used to determine molecular weight. The composition of the block copolymer was determined by ^{1}H NMR (400Hz, Varian MR-400) in deuterated chloroform at 5 mg/mL.

Tensile tests were performed at room temperature on the ARES-G2 rheometer (TA Instruments) and a special designed SER universal testing platform.[34,44] The strips used for tensile test have a dimension of 30 mm (length) ×8 mm (width) ×1 mm (thickness). The strain rate was 0.1 s^{-1}. All samples were stretched until breakage to collect ultimate tensile strength and elongation at break. The rheological measurements of the pre-cure compounds were performed on TA ARES-G2 rheometer at 25 °C, ω=6.28 rad/s. The aged samples were storage at room temperature for four months. The density measurements of the cured composites were performed according to ASTM D297-15. The TEM specimens with about 90 nm thickness were microtomed below −140 °C by cryo-ultramicrotomy (Leica Ultracut 125UCT). The morphological characterization was performed by JEOL 2100 scanning and transmission electron microscope at 200 kV.

RESULTS AND DISCUSSION

Molecular characterizations

The molecular characteristics of the polymeric materials are included in **Table 1**. The molecular weight of each block of the symmetric diBCP was chosen to be larger than the PDMS matrix and homoPS, which can induce the swelling of the diBCP by homopolymers,[45] and therefore promote the compatibilization. The molecular weight and polydispersity of the block copolymers and aliquots of PS were characterized via GPC, shown in **Figure S1**. The copolymer composition was calculated by ^{1}H-NMR spectroscopy in **Figure S2** and **Figure S3**. GPC traces of the products revealed the presence of some homoPS, corresponding to a terminated first block. The impurities in D_3 solution and THF may terminate part of living PS. The efficiency of diblock coupling is about 80%, so further fractionation was performed to remove homoPS and most of diBCP.[41,43] The dispersity of the final product reveals the high degree of molecular and compositional homogeneity.

Table 1: Molecular characteristics of neat PDMS, homopolystyrene and block copolymers

Sample	M_n(kg/mol)	M_w/M_n	$f_{PS\%}$	$w_{PS\%}$
Vinyl-terminated PDMS	28	1.57	–	–
Homopolystyrene (H)	23	1.52	–	–
PDMS-b-PS (D)	61	1.08	0.47	0.49
PS-b-PDMS-b-PS (T)	121	1.10	0.47	0.49

Number-average molecular weight and dispersity were determined by gel permeation chromatography. Volume and weight fraction calculated based on ^{1}H NMR results by using densities ρ_{PDMS}= 0.97 g/cm^3,[46] ρ_{PS}= 1.05 g/cm^3.[47]

Preliminary composition screening

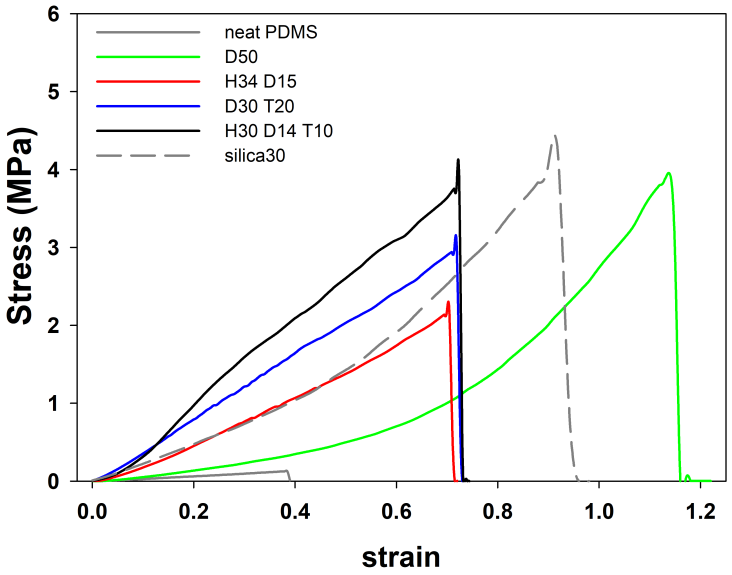

Figure 1: Representative stress-strain curves of neat PDMS, all-polymer and silica reinforced composites.(strain rate = 0.1 s^{-1}, room temperature) The number in sample code represents the weight fraction of the filler. For example, D50 represents the sample containing PDMS-b-PS 50 wt%.

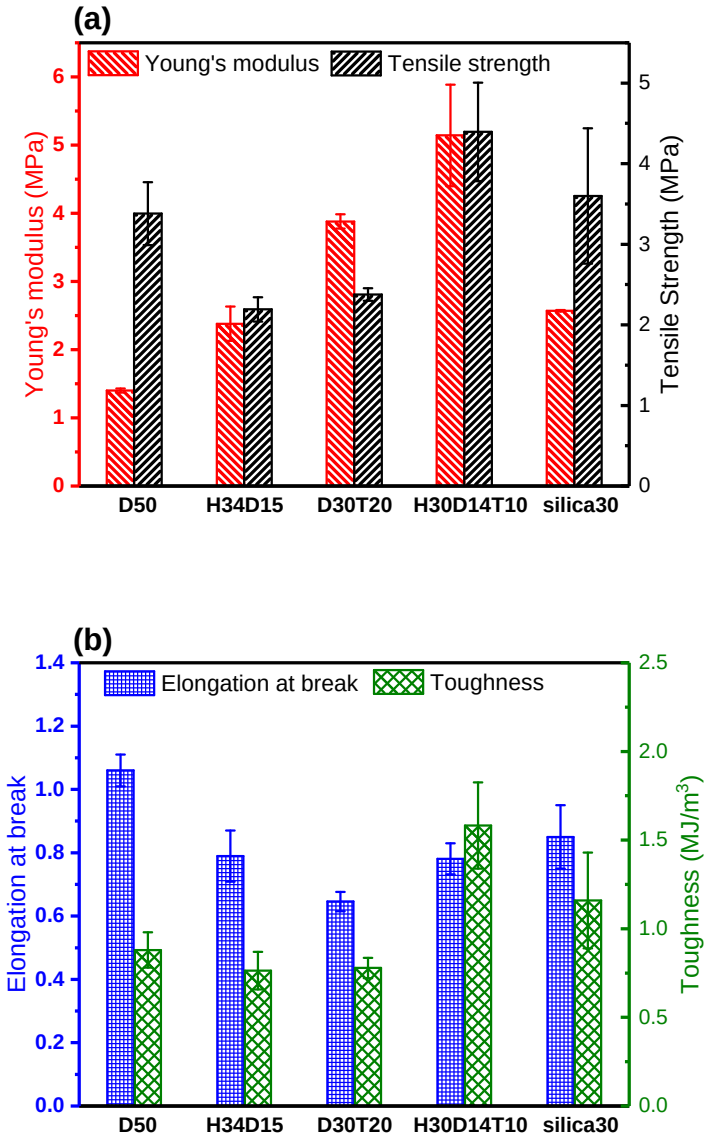

Figure 2: Mechanical properties of all-polymer and silica reinforced composites: (a) Young's modulus and tensile strength; (b) Elongation at break and toughness.

A preliminary screening of composition was performed to find the optimal one that brings the best mechanical performance. The constituent materials in **Table 1** were compounded, cured, and characterized. Composites are denoted by their mass composition, for example `D50` is 50 wt % diBCP (D), 50 wt % vinyl-terminated PDMS matrix; `H30 D14 T10` is 30 wt % homoPS (H), 14 wt% diBCP (D), and 10 wt % triBCP (T). The **Figure 1** shows

the representative stress-strain curves of neat PDMS, four all-polymer samples and the silica reinforced composites as the reference. The associated parameters including tensile strength, Young's modulus, elongation at break, and toughness are shown in **Figure 2** and the raw data are summarized in **Table S1**. Young′s modulus was calculated by linear regression within the elastic region of each curve. Toughness was determined by the integrated area under engineering stress-strain curve. The neat PDMS is apparently too weak to be serviceable without reinforcing filler. The silica content was set at 30 wt%, which is maximized to bring the best mechanical performance. It is limited by the processability due to the drastic viscosity increase.[48] At such content, silica/ PDMS blend shows a solid-like rheological response, which causes processing difficulties and platinum catalyst mixing. The details will be discussed in the following section.

The crosslinkable PDMS matrix content is kept near 50 wt%, corresponding to the optimized diBCP/PDMS composition we identified previously.[34] Since the PDMS blocks in diBCP and triBCP do not participate in the platinum-catalyzed cross-linking reaction, insufficient cross-linkable PDMS matrix content impairs the mechanical properties. We first investigated the compatibilizing effect of diBCP by the comparison between `D50` and `H34 D15`. While effective compatibilization has been reported at block copolymer content below 10 wt%,[35,36] we selected 15 wt% diBCP to fully saturate the PDMS/ PS interface; excess diBCP forms micelles and vesicles, still providing mechanical reinforcement. **Figure 2** shows that `H34 D15` features an increases Young's modulus compared to `D50`, at the expense of elongation-at-break, tensile strength, and tensile toughness. This tradeoff indicates that solely promoting the homoPS filler-matrix interaction by compatibilization with diBCP may not be sufficient.

Consequently, triBCP was added to diBCP composite to verify if the triblock copolymer can bring any potential additional reinforcement effect. Although the PS content of `D50` and D30 T20 is the same, the Young's modulus is 170% higher with triblock, while the other tensile properties were slightly reduced. This impact can be attributed to the additional block

connectivity of the triBCP that can provide additional strength, while also indicating that the triBCP chains may have different conformations, which are less resistant to deformation, from the diBCP in PDMS matrix. Thus, 10 wt% triBCP was added to homoPS/ diBCP composite to further verify the reinforcement effect of triBCP, which brings unexpected results. As shown in **Figure 2**, although only 10 wt% triBCP addition was made along with 4 wt% homoPS decrease, the mechanical properties of `H30 D14 T10` are boosted in comparison to `H34 D15`. Young's modulus, tensile strength, and tensile toughness are roughly doubled without reducing the elongation-at-break. Even compared to the silica composite, `H30 D14 T10` features twice the Young's modulus, larger tensile strength and toughness. Such results have confirmed the prominent reinforcing effect of `H30 D14 T10`, which has been investigated further by TEM in order to reveal the structure-property relationships.

Figure 3 shows representative TEM micrographs; natural contrast from the Si atom yields dark PDMS-rich domains and light for PS-rich areas. **Figure 3 (a)** shows that `D50` contains densely packed but not overlapped micelles and vesicles. The density of self-assembled fillers is such that there should be significant entanglement between the PDMS corona and the matrix, consistent with the exceptional mechanical performance of this specimen. Further increasing diBCP content is not effective, since the overlapped micelles decrease the concentration of PDMS homopolymer chains in the corona layers by the repulsive interaction energy of PS/ PDMS, which impairs the entanglement. On the other hand, the PS domains in PDMS/ diBCP blend are isolated from each other due to this repulsion. This bottleneck hints that improving the interaction between PS domains can be a more effective way to enhance mechanical properties. As expected, micelles and vesicles formed by the excess diBCP in the homoPS/ diBCP composite are shown in **Figure 3 (b)**, which indicates the possible saturation of diBCP at the PS/ PDMS interface. Moreover, the elongation at break decrease of homoPS/ diBCP composite may be caused by the increased interparticle distance compared to diBCP composite. `H 34 D15` also has larger average PS domain size than `D50`, which brings down the filler surface area and impairs the filler-matrix interaction.

The morphology of T20 was examined by TEM in **Figure 3 (c)** to isolate the self-assembly behavior of the triBCP architecture. Surprisingly, unlike D50 with sub-micron domain sizes even at 50 wt% loading, the miscibility of the triBCP with the matrix is poor such that macrophase-separated domains of a few microns are dominant. To form micelles may be entropically unfavorable compared to its placement in a lamellar domain. This illustrates that the dispersion of neat triBCP is poor compared to diBCP and suggests that its concentration should be limited to avoid macrophase separation.

In D30 T20 (**Figure 3 (d)**), the interface stabilizing character of diBCP alleviates the frustration in T20, facilitating the formation of micelles and vesicles. Evidently, the triBCP strongly partitions to the micelle interior per the proliferation of large onion-like multilayer vesicles. The condensed packed triBCP domains are broken by diBCP and have the transition of co-micellization with diBCP.[49] This change in morphology corresponds to the mechanical properties change compared to D50. The larger vesicle size leads to increased inter-particle distance, which causes decrease of elongation of break. On the other hand, singe multilayer vesicles may be more resistant to small-strain deformation than mono-layer vesicles, which contributes to the Young's modulus increase. Although the details of the comicellization were not investigated, the useful information has been provided that the dispersion of triBCP in PDMS can be promoted by the diBCP presence. As revealed by **Figure 3 (e)**, most of triBCP has dispersed and formed the vesicles with diBCP, which should favor mechanical reinforcement, while large isolated domains of triBCP can be still detected. Since most of diBCP resides at the PDMS/ PS interface to form micelles and vesicles, the rest diBCP may be insufficient for co-micellization with triBCP. However, further increasing the diBCP content will not improve the compatibilization since the compatibilizer has reached saturation. Therefore, optimized mechanical properties can be achieved by further reducing the triBCP content.

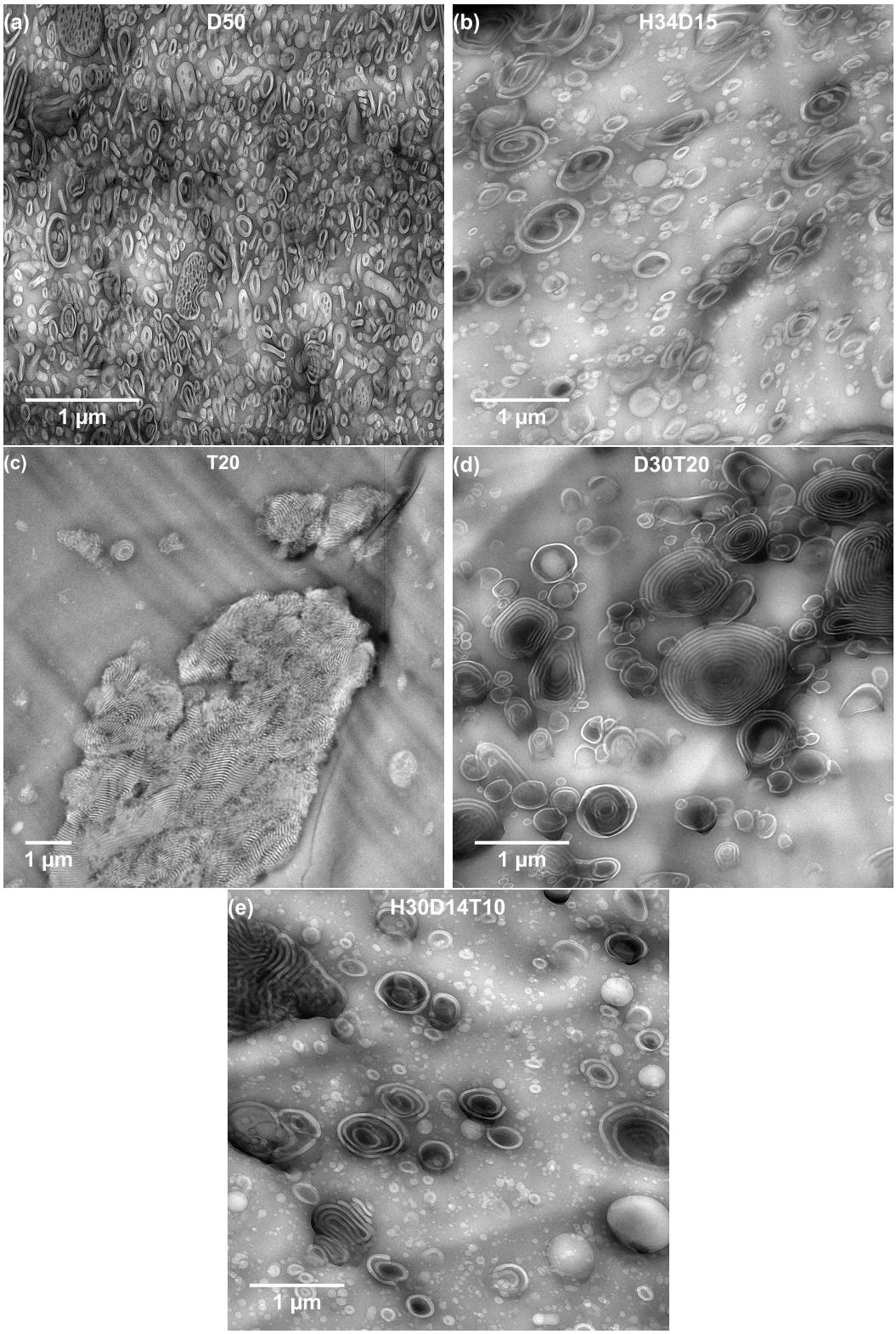

Figure 3: Representative TEM images of all-polymer composites: (a) D50; (b) H34 D15; (c) T20; (d) D30 T20; (e) H30 D14 T10.

Effect of triblock copolymer content on mechanical properties

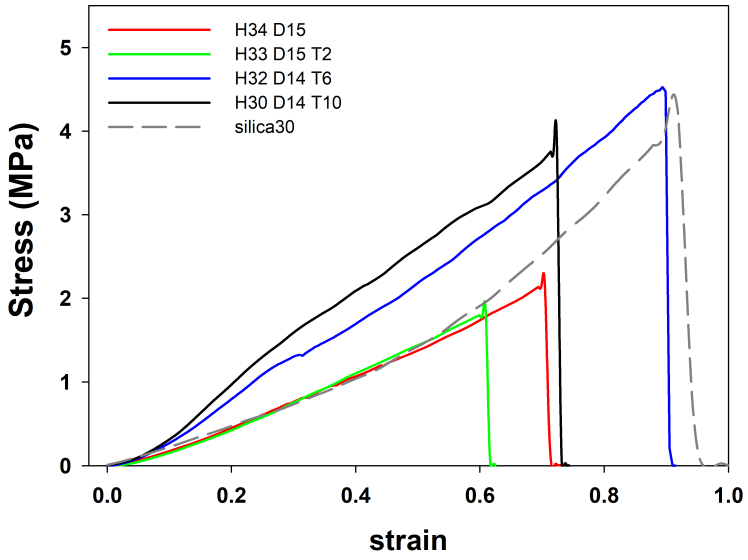

Figure 4: Representative stress-strain curves of all-polymer PDMS composites containing different loadings of triblock copolymer.(strain rate=0.1 s^{-1}, room temperature)

Based on the composition screening, the content of triBCP is lowered to investigate the effect of triBCP content on the mechanical properties of homoPS/ diBCP/ triBCP composite. **Figure 4** shows representative stress-strain curves as a function of triBCP content with silica-reinforced composite as the reference. The associated parameters including tensile strength, Young's modulus, elongation at break, and toughness are shown in **Figure 5** and summarized in **Table S2**. Overall, the addition of triBCP has a prominent impact on the mechanical properties since a dramatic change is brought by only small quantity of triBCP within 10 wt%. The first 2 wt% triBCP addition causes little reinforcing effect on Young's modulus and slight decrease of the rest three parameters. However, the 6 wt% addition causes a strong enhancement on mechanical properties by doubling the tensile strength and toughness, and bringing an 80% increase to the Young's modulus. The following increase to 10 wt% makes no further progress. Such behavior gives hint that the triBCP may form a network as described by percolation theory.[50] Below a certain value, fillers are too few to form the network. If the content continues increasing, the reinforcing effect (such as electrical

conductivity) will be intensified drastically when a critical filler content called percolation threshold is reached. In addition, a hypothesized schematic illustration based on the bridge/ loop chain conformations theory of triblock copolymer is shown in **Figure 6 (a)**, which illustrates the possible conformations of triBCP in the PDMS/ homoPS/ diBCP/ triBCP blends. Assuming all diBCP resides at the interface and no triBCP forms isolated domains: for a single triBCP chain, if both PS ends are attached on the same homoPS domain, the PDMS block will have a loop conformation; while if both PS ends are attached on different homoPS domains, the PDMS block will have a bridge conformation. In this case, no PS dangling ends should exist since the continuous phase is PDMS matrix and the PS ends should be forcedly attached to the PS phase due to thermodynamic repulsion. The bridge conformation is the major microstructure that promotes the connection between different PS domains to enhance the mechanical properties. Two entangled loops should also bring additional reinforcement, while if two loops are isolated, such effect does not exist.

`H33 D15 T2` mechanical data reveal that the triBCP content is below the percolation threshold. In addition, ineffective triBCP chains may form isolated loops that impair the existing diBCP compatibilization, weakening the mechanical properties. In `H32 D14 T6`, significantly improved mechanical properties indicate that the triBCP content should be above and close to the critical content. Most triBCP should form into bridges and loops rather than isolated large domains. As shown in the TEM micrograph **Figure 6 (b)**, no isolated triBCP domains are detected. The percolation network formed by the bridges and entangled loops provides the linkages between the PS domains and therefore enhances the mechanical properties. As for `H30 D14 T10`, the excess triBCP content does not bring much excess mechanical reinforcement. On the contrary, as discussed in previous subsection, the large, isolated triBCP domains may interrupt the percolation network and bring adverse effects to the mechanical properties. Overall, `H32 D14 T6` has the best mechanical performance, superior to the silica-filled reference, especially the Young's modulus, which is 60% higher.

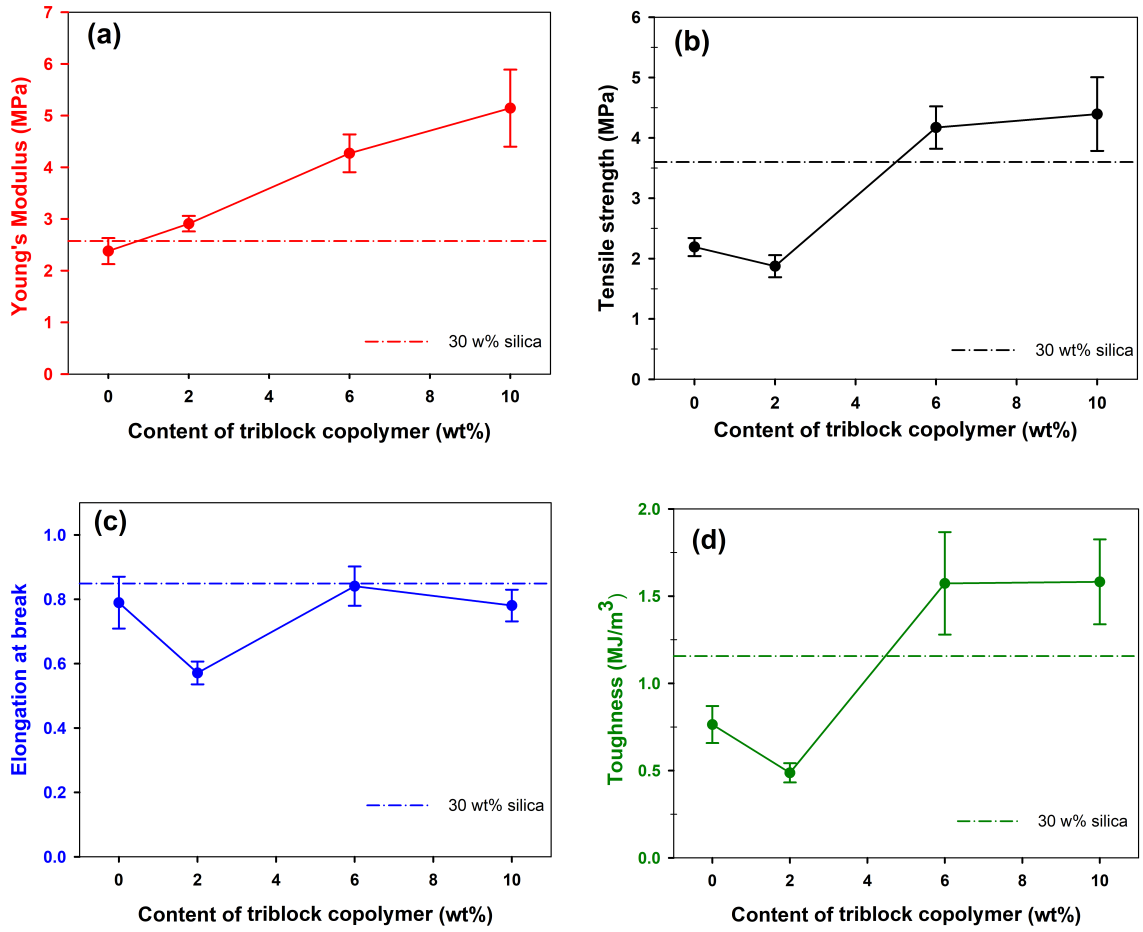

Figure 5: Effect of PS-PDMS-PS triblock copolymer content on mechanical properties and the comparison with 30 wt% silica filled PDMS composites—(a) Young's modulus (b) Tensile strength (c) Elongation at break and (d) Toughness.

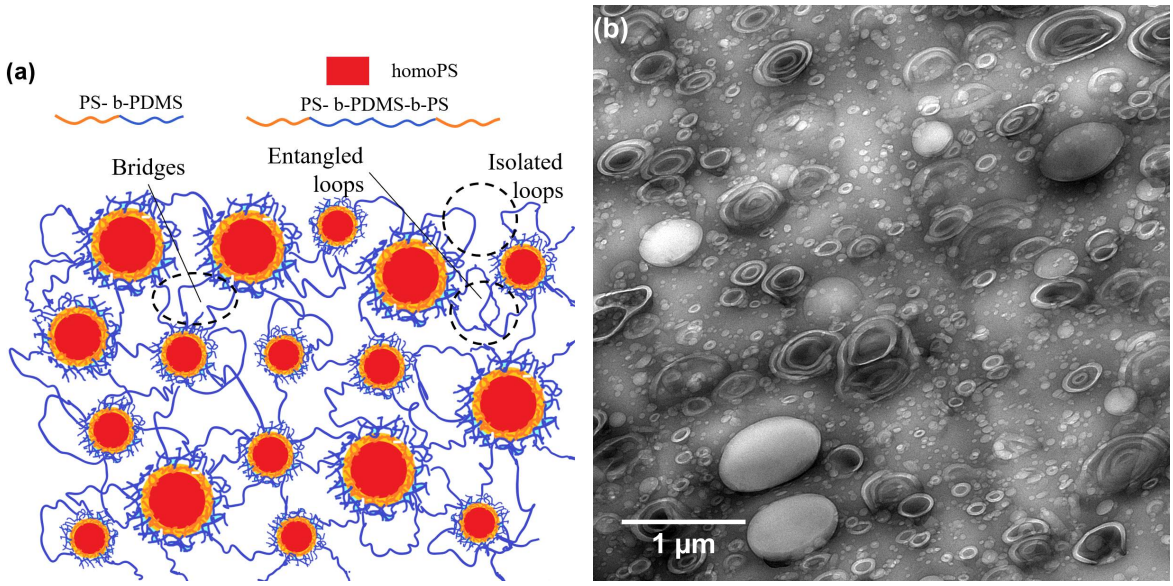

Figure 6: (a) Schematic illustration of the possible conformations of the PS-PDMS-PS triblock copolymer in PDMS/ homoPS/ PS-PDMS/ PS-PDMS-PS blends;
(b) Representative TEM image of 32 H/ 14 D/ 6 wt% T composite.

Rheological characterizations of the precured all-polymer and silica compounds

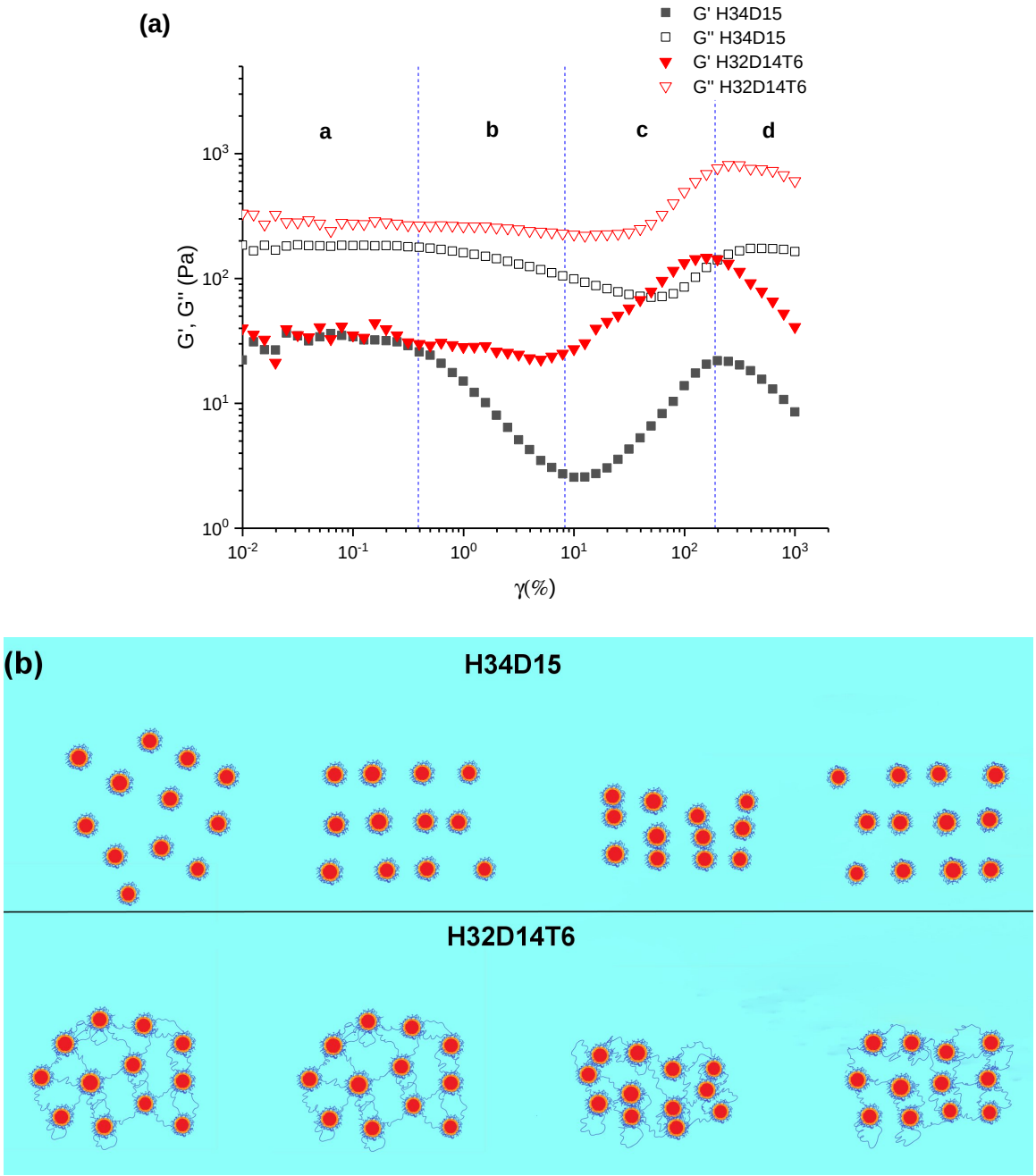

Figure 7: (a) Storage modulus (G') and loss modulus (G") of 34 H/ 15 wt% D and 32 H/ 14 D/ 6 wt% T compounds as a function of strain amplitude at 25 °C, 6.28 rad/s; (b) Schematic illustration of the probable microstructures at different stages of 34 H/ 15 wt% D and 32 H/ 14 D/ 6 wt% T compounds under large amplitude oscillatory shear (LAOS)

.

To further investigate the effect of triBCP addition on the rheological properties and microstructures, oscillatory strain-sweep shear tests were performed. The applied amplitude is increased at a fixed frequency and the viscoelastic response transforms from the linear region at small strain to the nonlinear region at large strain. Although the storage modulus (G') and loss modulus (G") are defined in linear region, the nominal values still retain the original correlation with viscoelasticity and are able to reveal the structure-property relationship due to shear thickening/ thinning by the large amplitude oscillatory shear (LAOS) behavior.[51] As shown in **Figure 7 (a)**, the modulus-strain curves of `H34 D15` and `H32 D14 T6` are divided into four stages depending on the variations of LAOS behavior. In **Stage a**, both compounds exhibit the Newtonian behavior with linearity at small strain, while in **Stage b**, the former one shows the shear thinning behavior but `H32 D14 T6` shows only a slight decrease in modulus. In **Stage c** and **Stage d**, G' and G" of both compounds have local maxima followed by decreasing. Such difference in oscillatory response provides the evidence that the triBCP addition strongly affects the rheological properties.

Based on the bridge/loop and percolation theories discussed above, and the LAOS behavior of an aqueous solution of PEO-PPO-PEO triblock copolymers reported by Hyun et al,[52] the probable mechanism of the complex behavior under LAOS is shown in **Figure 7 (b)**. Only homoPS dispersed phases are shown, while diBCP micelles are not shown. In **Stage a**, both compounds exhibit linear behavior since the shear force is not sufficient to change the microstructures of both compounds, which is indicated by the constant G' and G". In **Stage b**, the free fillers in the triBCP-free `H34 D15` tend to align to the flow direction, which weakens the obstruction along the flow direction and brings the strain thinning behavior. However, the fillers in the triBCP containing `H32 D14 T6` are constrained by the triBCP percolation network, which enhances the resistance to the shearing effect and suppresses the shear thinning behavior. In **Stage c**, the increased amplitude facilitates the fillers growing into clusters, because the PDMS coronae and loops tend to entangle with each other when the fillers are close enough during oscillation. The cluster formation increases the obstacles

in the flow directions and leads to both G' and G" increase. In **Stage d**, the amplitude reaches the value that is large enough to break up the clusters and align the fillers again to the flow direction, which is reflected by the second strain thinning.

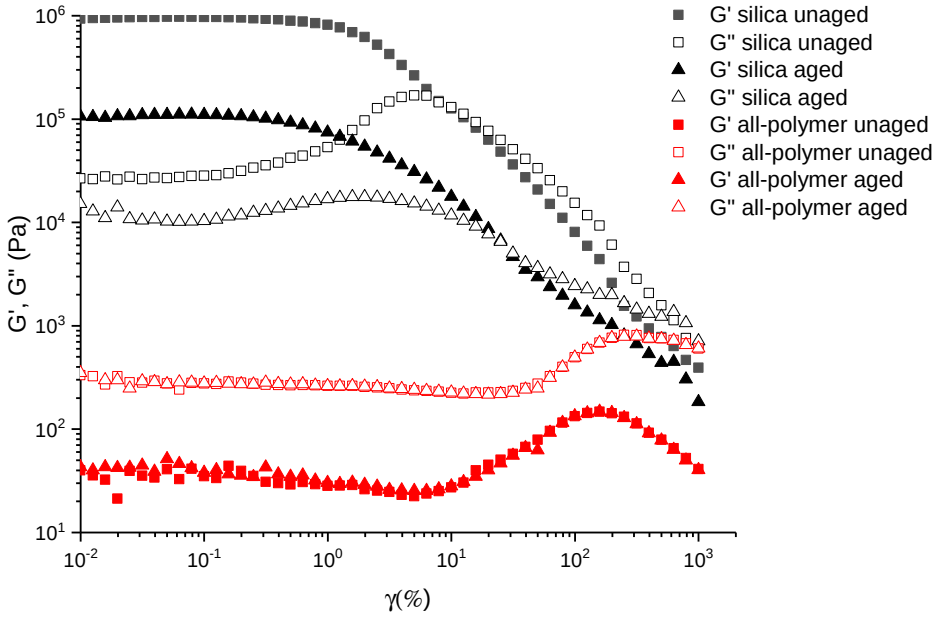

Figure 8: Influence of aging (four-month storage) on G' (solid symbols) and G" (hollow symbols) of silica (30 wt%) and all-polymer (H 32/ D 14/ T 6 wt%) compounds at 25 °C, 6.28 rad/s.

Figure 8 shows the influence of aging on the G' and G" of the precured silica and all-polymer compounds after four-months of storage under ambient conditions. The compound containing all-polymer fillers is apparently much easier to be processed, which is revealed by the large difference between the modulus of silica and all-polymer compounds. Increasing silica volume fraction induces the fluid-to-solid transition, which is caused by the hydrodynamics effect brought by the inclusion of rigid particles and intensified by matrix-filler interactions.[4,5] In addition, the transition is also led by the increased solid-like bound rubber layer due to the PDMS adsorption on silica surface, which is densely packed and insoluble in the matrix.[8,11] The solid-like behavior is also revealed by the G"/G' ratio, as G' is larger than G" at small strain. The necessity of strong external shearing force is indicated by the

shear-induced solid-to-liquid transition, as $\tan\delta$ increases above unity when the strain becomes higher. However, the all-polymer compound still exhibits liquid-like behavior without changing the fluid characteristics of PDMS and remains linear in a wide region.

Moreover, the months of storage decreases the modulus of the silica compound. As the PDMS chain adsorption onto the silica surface continues and the bound rubber content increases, the filler-filler and filler-matrix interactions are gradually replaced by the bound rubber layer. This aging phenomenon reorganizes the filler dispersion, especially the silica particles connected by the PDMS bridging chains.[11,12] The agglomeration deteriorates the percolation network and therefore lowers the modulus, whereas no conspicuous variation is detected from the all-polymer compound after the long-term storage. The morphological stability of all-polymer compound may be attributed to the thermodynamic repulsion between PS and PDMS phases. Furthermore, as shown in **Figure S4**, the density difference between silica and PDMS may also cause sedimentation within the suspension during the long-term storage, while the density difference of PDMS and PS is almost negligible, which causes that the all-polymer compound is more stable than the silica compound.

CONCLUSION

It has been shown that the homoPS along with symmetric PDMS-PS diblock and triblock copolymers can provide prominent reinforcement on the PDMS elastomer. After the screening of various polymeric fillers and additives, the symmetric PS-PDMS diblock copolymer is used as the compatibilizer to improve the filler dispersion and the PS-PDMS-PS triblock copolymer is added to promote the interaction between isolated PS domains. The prominent mechanical reinforcing effect of triBCP addition is confirmed by `H32 D14 T6`, which has the optimal mechanical properties. The 6 wt% addition of triBCP causes a strong enhancement on mechanical properties by doubling the tensile strength and toughness, and bringing an 80% increase to the Young's modulus, compared to the `H34 D15` composite. `H32 D14 T6` is

also superior to silica composite, especially the Young's modulus, which is 60% higher. The reinforcement may be brought by conformations of the triblock copolymers that connect different PS domains through bridges and entangled loops. It is revealed by the large amplitude oscillatory shear tests that the triBCP addition strongly affects the rheological properties and leads to the microstructure with stronger shearing resistance, further supporting the inference of interdomain connectivity. The aging effect that originates from PDMS chain adsorption on the filler particle surface is avoided since PS and PDMS are very thermodynamic repulsive.

Acknowledgement

This work is funded by the Department of Energy's Kansas City National Security Campus, operated by Honeywell Federal Manufacturing & Technologies, LLC, under contract number DE-NA0002839.

Supporting Information Available

Supporting Information. Synthetic route of PS precursor, block copolymers; GPC chromatographs of PS precursor, block copolymers; ^{1}H-NMR spectra of block copolymers; platinum catalyzed silicone crosslinking (hydrosilylation reaction); summary table of mechanical properties of neat PDMS, all-polymer and silica reinforced composites; Summary table of mechanical properties of all-polymer composites with various triblock copolymer content; density comparison of the raw materials, all-polymer and silica composites.

References

(1) Warrick, E. L.; Pierce, O. R.; Polmanteer, K. E.; Saam, J. C. Silicone Elastomer Developments 1967-1977. *Rubber Chem. Technol.* **1979**, *52*, 437–525.

(2) Boonstra, B. B. Role of particulate fillers in elastomer reinforcement: a review. *Polymer* **1979**, *20*, 691–704.

(3) Camenzind, A.; Schweizer, T.; Sztucki, M.; Pratsinis, S. E. Structure & strength of silica-PDMS nanocomposites. *Polymer* **2010**, *51*, 1796–1804.

(4) Aranguren, M. I.; Mora, E.; MACOSKO, C. W. Compounding Fumed Silicas into Polydimethylsiloxane: Bound Rubber and Final Aggregate Size. *J. Colloid Interface Sci.* **1997**, *195*, 329–337.

(5) Shim, S. E.; Isayev, A. I. Rheology and structure of precipitated silica and poly(dimethyl siloxane) system. *Rheol Acta* **2004**, *43*, 127–136.

(6) Aranguren, M. I.; Mora, E.; DeGroot, J. V.; Macosko, C. W. Effect of reinforcing fillers on the rheology of polymer melts. *J. Rheol.* **1992**, *36*, 1165–1182.

(7) Boonstra, B. B.; Cochrane, H.; Dánnenberg, E. M. Reinforcement of Silicone Rubber by Particulate Silica. *Rubber Chem. Technol.* **1975**, *48*, 558–576.

(8) Yue, Y.; Zhang, C.; Zhang, H.; Zhang, D.; Chen, X.; Chen, Y.; Zhang, Z. Rheological behaviors of fumed silica filled polydimethylsiloxane suspensions. *Composites Part A* **2013**, *53*, 152–159.

(9) Cohen-Addad, J. P.; Roby, C.; Sauviat, M. Characterization of chain binding to filler in silicone-silica systems. *Polymer* **1985**, *26*, 1231–1233.

(10) DeGroot, J. V.; Macosko, C. W. Aging Phenomena in Silica-Filled Polydimethylsiloxane. *J. Colloid Interface Sci.* **1999**, *217*, 86–93.

(11) Ma, T.; Yang, R.; Zheng, Z.; Song, Y. Rheology of fumed silica/polydimethylsiloxane suspensions. *J. Rheol.* **2017**, *61*, 205–215.

(12) Selimovic, S.; Maynard, S. M.; Hu, Y. Aging effects of precipitated silica in poly(dimethylsiloxane). *J. Rheol.* **2007**, *51*, 325–340.

(13) Vondráček, P.; Schätz, M. Bound rubber and "crepe hardening" in silicone rubber. *J. Appl. Polym. Sci.* **1977**, *21*, 3211–3222.

(14) Schnurrbusch, K.; Kniege, W. Structure control additive for convertible organopolysiloxanes, and preparation thereof. 1970; US Patent 3,551,382.

(15) Cochrane, H.; Lin, C. S. The Influence of Fumed Silica Properties on the Processing, Curing, and Reinforcement Properties of Silicone Rubber. *Rubber Chem. Technol.* **1993**, *66*, 48–60.

(16) Dong, J.; Liu, Z.; Cao, X.; Zhang, C. Elastomers based on α,ω-dihydroxy-polydimethylsiloxane/polystyrene blends: Morphology and mechanical properties. *J. Appl. Polym. Sci.* **2006**, *101*, 2565–2572.

(17) Dong, J.; Liu, Z.; Han, N.; Wang, Q.; Xia, Y. Preparation, morphology, and mechanical properties of elastomers based on α,ω-dihydroxy-polydimethylsiloxane/polystyrene blends. *J. Appl. Polym. Sci.* **2004**, *92*, 3542–3548.

(18) Dong, J.; Zhang, N.; Liu, Z. Preparation, morphology, and mechanical properties of elastomers based on polydimethylsiloxane/ polystyrene blends. *J. Appl. Polym. Sci.* **2009**, *112*, 985–990.

(19) Fu, F.-S.; Mark, J. E. Elastomer reinforcement from a glassy polymer polymerized in situ. *J. Polym. Sci., Part B: Polym. Phys.* **1988**, *26*, 2229–2235.

(20) Wang, S.; Mark, J. E. Reinforcement of elastomeric poly(dimethylsiloxane) by glassy poly(diphenylsiloxane). *J Mater Sci* **1990**, *25*, 65–68.

(21) Tazawa, S.; Shimojima, A.; Maeda, T.; Hotta, A. Thermoplastic polydimethylsiloxane with l-phenylalanine-based hydrogen-bond networks. *J. Appl. Polym. Sci.* **2018**, *135*, 45419.

(22) Wang, S.; Mark, J. E. Generation of glassy ellipsoidal particles within an elastomer by in situ polymerization, elongation at an elevated temperature, and finally cooling under strain. *Macromolecules* **1990**, *23*, 4288–4291.

(23) Sinturel, C.; Bates, F. S.; Hillmyer, M. A. High χ-Low N Block Polymers: How Far Can We Go? *ACS Macro Lett.* **2015**, *4*, 1044–1050.

(24) Hsieh, I.-F.; Sun, H.-J.; Fu, Q.; Lotz, B.; A. Cavicchi, K.; Cheng, S. Z. D. Phase structural formation and oscillation in polystyrene- block -polydimethylsiloxane thin films. *Soft Matter* **2012**, *8*, 7937–7944.

(25) Wadley, M. L.; Hsieh, I.-F.; Cavicchi, K. A.; Cheng, S. Z. D. Solvent Dependence of the Morphology of Spin-Coated Thin Films of Polydimethylsiloxane-Rich Polystyrene-block-Polydimethylsiloxane Copolymers. *Macromolecules* **2012**, *45*, 5538–5545.

(26) Pa, N. F. C.; Ahmed, I.; Nawawi, M. G. M.; Abd Rahman, W. A. W. Influence of polystyrene on PDMS IPNs blend membrane performance. *Separation Science and Technology* **2012**, *47*, 562–576.

(27) Dewasthale, S.; Shi, X.; Hablot, E.; Graiver, D.; Narayan, R. Interpenetrating polymer networks derived from silylated soybean oil and polydimethylsiloxane. *Journal of Applied Polymer Science* **2013**, *130*, 2479–2486.

(28) Dewasthale, S.; Graiver, D.; Narayan, R. Biobased interpenetrating polymers networks derived from oligomerized soybean oil and polydimethylsiloxane. *Journal of Applied Polymer Science* **2015**, *132*.

(29) Cochran, E. W.; Williams, R. C.; Hernandez, N.; Cascione, A. Thermoplastic elastomers via reversible addition-fragmentation chain transfer polymerization of triglycerides. 2018; US Patent 10,093,758.

(30) Hernández, N.; Yan, M.; Williams, R. C.; Cochran, E. *Green Polymer Chemistry: Biobased Materials and Biocatalysis*; ACS Symposium Series; American Chemical Society, 2015; Vol. 1192; pp 183–199.

(31) Holden, G. In *Rubber Technology*; Morton, M., Ed.; Springer US, 1987; pp 465–481.

(32) Saam, J. C.; Fearon, F. W. G. Properties of Polystyrene-Polydimethylsiloxane Block Copolymers. Colloidal and Morphological Behavior of Block and Graft Copolymers. 1971; pp 75–84.

(33) SAAM, J. C.; WARD, A. H.; FEARON, F. W. G. *Polymerization Reactions and New Polymers*; Advances in Chemistry; AMERICAN CHEMICAL SOCIETY, 1973; Vol. 129; pp 239–247.

(34) Shen, L.; Wang, T.-p.; Lin, F.-Y.; Torres, S.; Robison, T.; Kalluru, S. H.; Hernández, N. B.; Cochran, E. W. Polystyrene-block-Polydimethylsiloxane as a Potential Silica Substitute for Polysiloxane Reinforcement. *ACS Macro Lett.* **2020**, *9*, 781–787.

(35) Chuai, C. Z.; Li, S.; Almdal, K.; Alstrup, J.; Lyngaae-Jørgensen, J. The effect of compatibilization and rheological properties of polystyrene and poly(dimethylsiloxane) on phase structure of polystyrene/poly(dimethylsiloxane) blends. *J. Polym. Sci., Part B: Polym. Phys.* **2004**, *42*, 898–913.

(36) Marić, M.; Macosko, C. W. Block copolymer compatibilizers for polystyrene/poly(dimethylsiloxane) blends. *J. Polym. Sci., Part B: Polym. Phys.* **2002**, *40*, 346–357.

(37) Cigana, P.; Favis, B.; Jérôme, R. Diblock copolymers as emulsifying agents in polymer blends: Influence of molecular weight, architecture, and chemical composition. *Journal of polymer science part B: Polymer physics* **1996**, *34*, 1691–1700.

(38) Van Hemelrijck, E.; Van Puyvelde, P.; Macosko, C. W.; Moldenaers, P. The effect of block copolymer architecture on the coalescence and interfacial elasticity in compatibilized polymer blends. *J. Rheol.* **2005**, *49*, 783–798.

(39) Kalluru, S. H.; Hernandez, N.; Cochran, E. W. Reagent purification systems, methods, and apparatus. 2020; US Patent 10,532,964.

(40) Bajaj, P.; Varshney, S. K.; Misra, A. Block copolymers of polystyrene and poly(dimethyl siloxane). I. Synthesis and characterization. *J. Polym. Sci., Polym. Chem. Ed* **1980**, *18*, 295–309.

(41) Chu, J. H.; Rangarajan, P.; Adams, J. L.; Register, R. A. Morphologies of strongly segregated polystyrene-poly(dimethylsiloxane) diblock copolymers. *Polymer* **1995**, *36*, 1569–1575.

(42) Saam, J. C.; Gordon, D. J.; Lindsey, S. Block Copolymers of Polydimethylsiloxane and Polystyrene. *Macromolecules* **1970**, *3*, 1–4.

(43) Zilliox, J. G.; Roovers, J. E. L.; Bywater, S. Preparation and Properties of Polydimethylsiloxane and Its Block Copolymers with Styrene. *Macromolecules* **1975**, *8*, 573–578.

(44) Sentmanat, M. L. Miniature universal testing platform: from extensional melt rheology to solid-state deformation behavior. *Rheol Acta* **2004**, *43*, 657–669.

(45) Behling, R. E.; Wolf, L. M.; Cochran, E. W. Hierarchically Ordered Montmorillonite Block Copolymer Brushes. *Macromolecules* **2010**, *43*, 2111–2114.

(46) Kataoka, T.; Ueda, S. Viscosity-molecular weight relationship for polydimethylsiloxane. *J. Polym. Sci., Part B: Polym. Lett.* **1966**, *4*, 317–322.

(47) Fox, T. G.; Flory, P. J. Second-Order Transition Temperatures and Related Properties of Polystyrene. I. Influence of Molecular Weight. *J. Appl. Phys.* **1950**, *21*, 581–591.

(48) Cassagnau, P. Melt rheology of organoclay and fumed silica nanocomposites. *Polymer* **2008**, *49*, 2183–2196.

(49) Koňák, C.; Helmstedt, M. Comicellization of Diblock and Triblock Copolymers in Selective Solvents. *Macromolecules* **2003**, *36*, 4603–4608.

(50) Tu, C.; Nagata, K.; Yan, S. Morphology and electrical conductivity of polyethylene/polypropylene blend filled with thermally reduced graphene oxide and surfactant exfoliated graphene. *Polym. Compos.* **2017**, *38*, 2098–2105.

(51) Hyun, K.; Wilhelm, M.; Klein, C. O.; Cho, K. S.; Nam, J. G.; Ahn, K. H.; Lee, S. J.; Ewoldt, R. H.; McKinley, G. H. A review of nonlinear oscillatory shear tests: Analysis and application of large amplitude oscillatory shear (LAOS). *Prog. Polym. Sci.* **2011**, *36*, 1697–1753.

(52) Hyun, K.; Nam, J. G.; Wilhellm, M.; Ahn, K. H.; Lee, S. J. Large amplitude oscillatory shear behavior of PEO-PPO-PEO triblock copolymer solutions. *Rheol Acta* **2006**, *45*, 239–249.

Graphical TOC Entry